NOVEL ALL-SOLID-STATE SOIL NUTRIENT SENSOR USING NANOCOMPOSITE OF POLY(3-OCTYL-THIOPHENE) AND MOLYBDENUM SULFATE

Md. Azahar Ali[1], Xinran Wang[1], Yuncong Chen[1], Yueyi Jiao[1], Michael J. Castellano[1], James C. Schnable[2], Patrick S. Schnable[1], and Liang Dong[1]
[1]Iowa State University, Ames, IA, USA
[2]University of Nebraska-Lincoln, Lincoln, NE, USA

ABSTRACT

Nitrate is a major macronutrient for plant growth. There is a high demand to develop robust, reliable, and maintenance-free soil sensors for long-term monitoring of nitrate variations in field. An ion-selective membrane-based solid-state nitrate sensor is developed using poly(3-octyl-thiophene)-molybdenum disulfide nanocomposite as an ion-to-electron transducing layer. The sensor offers a high sensitivity of 64 mV/decade, a dynamic range of 1–1500 ppm NO_3^--N, and an improved selectivity for nitrate detection in soils. The sensor has demonstrated the ability to continuously monitor soil nitrate concentrations over a period of four weeks.

KEYWORDS

All-solid-state sensor, soil sensor, nanocomposite, ion-to-electron transducing layer

INTRODUCTION

After water, soil nitrogen (N) is the most limiting factor for plant growth. Crop productivity relies heavily on N fertilization [1]. At present N fertilizer is not efficiently assimilated by crops. Excess N fertilizer leaks into the environment, leading to significant negative environmental impacts on water quality, biodiversity, and atmospheric pollution. Continuous monitoring of nitrate dynamics in crop fields provides us maximum control over fertilizer management. Laboratory measurement of soil nitrogen is time-consuming and labor intensive. Remote sensors and on-the-go vehicle-based sensors have been used for in-field measurement of soil nitrate [1][2]. Accurate, long-term and field deployable nitrate sensors are still challenging.

Ion-selective membrane (ISM)-based potentiometric sensors are widely used to detect nitrate in water [3]. But, due to the necessity of using inner-filling solutions, conventional ISM-based nitrate sensors lack portability and long-term deployability [4]. Efforts have been made to develop all-state-solid sensors by introducing solid-contact ion-to-electron transducing materials, such as carbon nanotube [5], polypyrrole [6] and graphene [7], between the ISM and an electron conducting layer of the sensor. A desired solid-contact ion-to-electron transducing material requires both high redox property and hydrophobicity to increase stability, selectivity, and sensitivity.

This paper reports an all-solid-state potentiometric sensor for continuous monitoring of soil nitrate levels. The sensor uses a novel nanocomposite of poly(3-octyl-thiophene) (POT) and two-dimensional transition metal dichalcogenides of molybdenum disulfide (MoS_2) sheets as a solid-contact ion-to-electron transducing layer. POT has an excellent redox property but its electrical conductivity is low. MoS_2 sheets can provide a larger surface area, high conductivity, insensitivity to light or pH, and absence of possible side-reactions. The working electrode (WE) of the sensor is built on top of a copper pad of printed circuit board (PCB) covered by a patterned thin Au layer, a POT-MoS_2 nanocomposite-based solid-contact layer, and a nitrate-specific ISM. The incorporation of MoS_2 into POT can not only increase redox properties of POT, but also provide high hydrophobicity to minimize the formation of water thin layer between the ISM and metallic electron conduction layer. Generally, a notorious thin water layer is often formed at the interface between the ISM and conducting metal layer, acting as an interfacial barrier to fast electron transfer and negatively impacting selectivity of the sensor because different ions may be trapped inside this water layer. In our case, due to high hydrophobilicity, the POT-MoS_2 can counter the issue with the trapped water layer, contributing to increasing charge transfer and ion selectivity of the sensor. The reference electrode (RE) of the sensor includes a silver/silver chloride (Ag/AgCl) electrode covered by a proton exchange membrane to reduce redox reaction-induced chloride leaching from the RE, contributing to minimizing drift of reference potential.

The presented sensor is featured with an all-solid-state design that incorporates the POT-MoS_2 nanocomposite for improved device performance. It should be noted that the sensor is embedded in soil for continuous monitoring of nitrate dynamics for about four weeks.

DEVICE FABRICATION

This sensor was made on a PCB with two electrodes wherein one served as a WE and the other as thea RE. To functionalize the WE, POT and MoS_2 with a weight ratio of 1:4 (concentration of POT: 2.6 mg/mL) were dispersed in tetrahydrofuran. This composite solution was coated on a 4 mm-diameter circular Au using a high-precision liquid dispensing machine (Fig. 1a), and then dried at room temperature. After that, a nitrate-specific ISM was coated on the POT-MoS_2 layer and then conditioned in a 1500 ppm NO_3^--N solution for 24 hr.

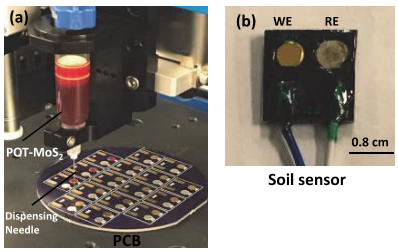

Figure 1: (a) Coating POT-MoS_2 nanocomposite on the surface of substrate using a programmable robotic dispensing system. (b) Photo of a fabricated nitrate sensing unit.

For the RE, Ag/AgCl paste was screen-printed on a silver layer and then dried at 110° C for 2 hr. A perfluorinated polymer, Nafion, was then coated on the surface of Ag/AgCl. The Nafion layer was dried at 90° C for 1 hr. The role of Nafion is to prevent redox reaction-induced chloride leaching from the Ag/AgCl material to increase potential stability at the RE.

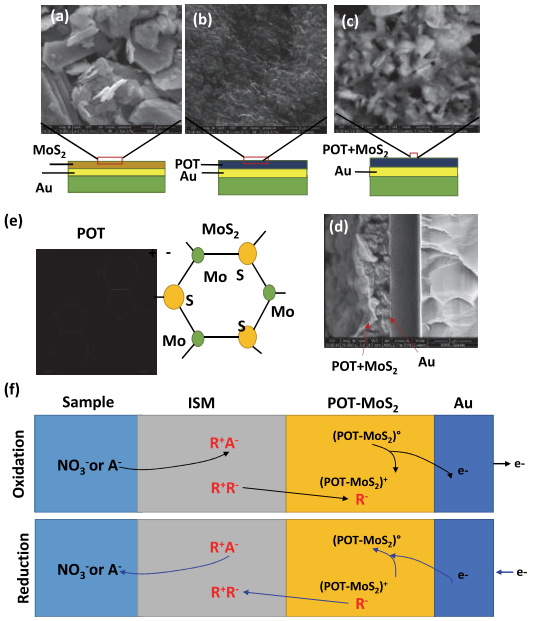

Figure 2: SEM for MoS_2 sheets (a), POT (b), and POT-MoS_2 materials (c) with schematic of various layers. (d) A cross-sectional view of POT-MoS_2/Au. (e) Molecular structure of POT and MoS_2. (f) The oxidation and reduction for printed WE (ISM/POT-MoS_2/Au) in presence of soil NO_3^- ions. R^+ and R^- represent anion and cation exchangers at organic membrane, and A^- are hydrophilic ions.

Figure 2 shows the scanning electron microscopic (SEM) images for MoS_2 sheets (a), POT (b), and POT-MoS_2 (c) with schematics of different structural layers. Image (a) shows MoS_2 sheets with a combination of large (> 1 µm) and small (< 1 µm) sheets. The observed porous morphology of POT is useful for forming a composite with MoS_2 (image b). In the POT-MoS_2 composite, MoS_2 is covered by POT maybe due to the oppositely charged interactions. A morphological transition of POT and MoS_2 indicate the formation of POT-MoS2 composite (image c). The POT-MoS_2 is ~1 µm thick (image d). Figure 2e shows a schematic presentation and molecular structure of both POT and MoS_2.

Figure 2f shows the ion exchange mechanism of the sensor for nitrate detection. The redox reaction is given by:

$$P^+_{(p)} + e^- + R^-(p) + NO_3^-{}_{(m)} \leftrightharpoons P_{(p)} + R^-_{(m)} + NO_3^-{}_{(aq)} \quad (1)$$

where m, p, and aq represent the ISM phase, POT-MoS_2 nanocomposite phase, and aqueous phase, respectively, and $P_{(p)}$ and $P^+_{(p)}$ represent a few monomeric units of the POT-MoS_2 in the neutral insulating state, and the oxidized state with polaronic sites, respectively. The movement of anions or cations, with the help of specific binding sites, produces a potential difference. E depends on the logarithm of the ion activity and described by Nernst equation,

$$E = E_0 + E_1 = E_0 + \frac{RT}{zF} \ln a_I(I) \quad (2)$$

where $a_I(I)$, R, T, z and F are the primary ion activity without any interfering, ions gas constant, temperature, charge in target ion, and Faraday constant, respectively. E_0 and E_1 are the constant potential at the RE and the potential devolved at the WE, respectively.

EXPERIMENTAL RESULTS

Electrochemical studies

The cyclic voltammetry (CV) studies (Fig. 3a) show that the POT-MoS_2-based sensor exhibited a higher redox current and peak-to-peak potential, compared to the POT-based electrode. The conductive nature of MoS_2 results in an increase in electron transfer. When incorporating the ISM, the redox current of the POT-MoS_2 decreased due to the insulating nature of ISM. The negatively charged ISM may repel ferro/ferricyanide molecules, thus reducing electron transfer.

The weight ratio of POT and MoS_2 was optimized (Fig. 3b) using the CV method wherein the peak-to-peak potential (ΔE) was calculated for the POT-MoS_2 electrode by varying MoS_2 concentration in the composite. At 1:4 weight ratio of POT and MoS_2, the ΔE was found to reach maximum. Measurement results for open circuit potential (OCP) of three electrodes (coated with MoS_2, POT or POT-MOS_2 and a nitrate-specific ISM) are shown in the inset of Fig. 3b. The OCP for the POT-MOS_2-based electrode (-327 mV) was shown higher than that for the POT- (-263 mV) and the MOS_2-based (-63 mV) electrodes. As evident in the CV studies, the POT-MoS_2 electrode shows a high redox capacitance property and redox electroactivity, allowing selective uptaking or release of hydrophilic NO_3^- ions.

Nitrate detection in standard solution

Nitrate detection was investigated for all the sensors using MoS_2, POT and POT-MoS_2 as different solid-contact materials. A home-made circuit was used to read out the OCP values as a function of concentration from 1 to 1500 ppm NO_3^--N. As the concentration changed, OCP would change. Figure 4a shows the output voltages for different WEs when responding to different nitrate concentrations. The corresponding calibration curves for the sensors are shown in Fig. 4b. The sensor using the POT-MoS_2 shows a higher sensitivity (64 mV/dec) with a wide dynamic range of 1 to 1500 ppm NO_3^--N, compared to that using POT (48 mV/dec) or MoS_2 alone (38 mV/dec).

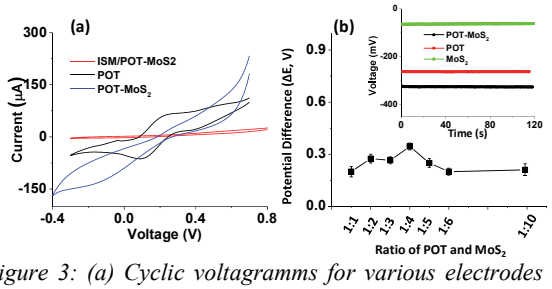

Figure 3: (a) Cyclic voltagramms for various electrodes in presence of standard PBS solution. (b) Ratio optimization for POT and MoS_2. Inset shows the voltages of all three electrodes after coated with nitrate-selective membrane in presence of 1000 ppm NO_3^--N.

Figure 4c shows the effect of environmental chloride ions on the ability of the POT-MoS_2-based sensor to detect nitrate ions. The result shows that the sensor was little affected by low-concentration Cl^- ions (e.g., 0.01 M and 0.1 M) in the nitrate solution. However, with extreme high Cl- concentrations such as 0.5 M and 1 M, the sensor output was deviated by ±2.2% and ±4.0%, respectively, from the output without any interfering ions. The potential drift may be caused by the non-selective interaction of the sensor with Cl^- ions in the ISM. Additional selectivity studies (Fig. 4d) of the different sensors were performed in presence of interfering anions such as phosphate (PO_4^{3-}), bicarbonate (HCO_3^-), and sulphate (SO_4^{2-}). The result shows that the POT-based or MoS_2-based sensor shows low selectivity, compared to the POT-MoS_2-based sensor.

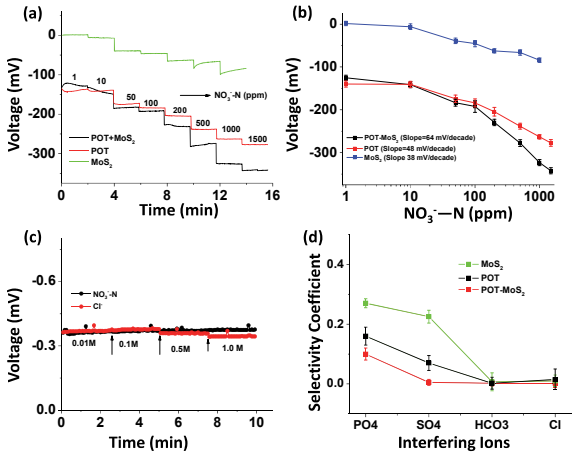

Figure 4: Responses to varying nitrate concentrations of standard nitrate solutions for MoS_2-, POT- and POT-MoS_2-based sensors (a) and corresponding calibration curves (b). (c) Effect of Cl^- ions on voltage output of the POT-MoS_2-based sensor. (d) Selectivity studies. The nitrate concentration was set to 100 ppm NO_3^--N and the interfering ions were set to 400 ppm. The selectivity coefficients were calculated using separate solution method.

Nitrate detection in soil

The POT-MoS_2-based nitrate sensor was applied to measure nitrate concentrations in extracted soil solutions collected from a corn field in Ames, Iowa. The readings from this sensor were compared with those from a commercial nitrate sensor (Laque Horiba). Our sensor measurement results agreed well with those obtained using the commercial sensor (Fig. 5a).

Two POT-MoS_2-based sensors were fixed on the walls of two column beakers filled with soil slurries (Fig. 5b-c). The beaker was 6 cm in diameter and 10 cm in height, and was loaded with mineral soils till 9 cm height from the bottom of the beaker. Small drain holes were created at the bottom. Each sensor was located at 7 cm from the bottom. During the measurement, the soil in one beaker was flushed with alternating solutions of 0 and 50 ppm NO_3^--N at different times, each time lasting 2 minutes, while the soil in the other beaker was flushed with 0 and 100 ppm NO_3^--N. Fig. 5d shows the outputs of the two sensors. When the soil was flushed with water (0 ppm), the output voltage of the sensor reached the -110 mV voltage baseline. When the soil was treated with the 50 ppm and 100 ppm NO_3^--N solutions, one sensor output went down to -123 mV, while the other to -150 mV, respectively. Fig. 5e shows the nitrate levels converted from the output voltages of the sensors.

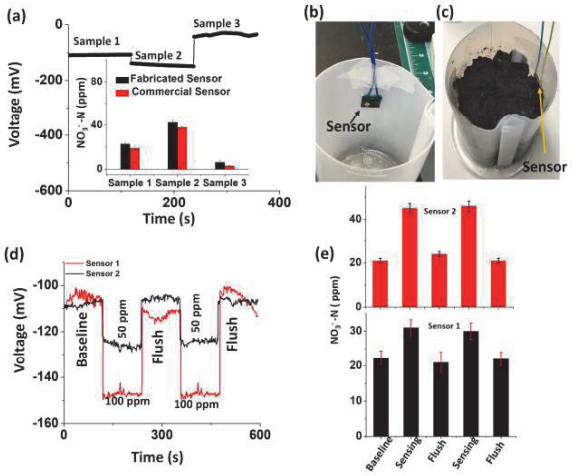

Figure 5: (a) Nitrate sensing for extracted soil solutions and validated using a commercial sensor. (b-c) Experimental setup. (d) Short-term soil nitrogen sensing in the soil column, where the baseline was set in the presence of water (baseline), and the column was flushed with DI water after the soil was treated with 100 and 50 ppm of NO_3^--N, and (e) Plot for corresponding sensor readings.

For long-term measurement, two sensors (sensor 1 and sensor 2) were deployed directly in soil slurries for ~27 days with different rates of nitrate concentration (50 and 100 ppm NO_3^--N) (Fig. 6a-b). For the sensor 1, when the beaker (without holes at the bottom) was treated with water, NO_3^--N was found to be ~14-23 ppm (Fig. 6c). Due to the slow diffusion of pre-occurrence nitrate ions from the soil slurry into water, the nitrate concentration slowly increased until a maximum concentration was reached. Further, the sensor showed a gradual decrease in concentration in a range of 2-5 ppm NO_3^--N due to slow evaporation. In this parched soil condition, the nitrate concentration was found to be almost constant. Upon further repeating the experiment two times, the sensor showed similar results.

Interestingly, when the 50 ppm of NO_3^--N was poured into the soil beaker, sensor 1 began to show a slow increase in NO_3^--N, and reached a maximum value of 53 ppm NO_3^--N. With the addition of external nitrate into the soil, the sensor took approximately 3 h to reach a maximum nitrate level, indicating slow diffusion of nitrate ions into the soil. This is because when soil particles at the sensor interface are completely wet, nitrate ions may diffuse slowly from the external nitrate solution (as we filled the beaker) due to the concentration gradient. The NO_3^--N concentration was further decreased to a low value of 2–5 ppm when the soil particles became parched due to water evaporation, which restricted the mobility of the nitrate ions. Sensor 1 showed an almost similar performance of NO_3^--N, while the sensor was further flushed with 50 ppm NO_3^--N concentration another three times. When more water containing NO_3^--N (see the last two repeated measurements, Fig. 8c) was

poured, the sensor showed a longer nitrate response at 50 ppm, as the evaporation of water from the soil takes time.

Similarly, for sensor 2, the performance was studied in the presence of 0 ppm (water) and 100 ppm of NO_3^--N concentration for 2 weeks (Fig. 6d), and the sensor was kept in parched soil conditions for another 2 weeks (Fig. 6e). With water filling, the sensor exhibited a concentration of approximately 20–25 ppm of NO_3^--N due to the pre-existing nitrate ions in the soil. Further, the soil water content dried slowly, and the soil became parched under this condition. The sensor showed a similar NO_3^--N response as was observed in the case of sensor 1. When the soil slurry was flushed with 100 ppm NO_3^--N solution, the output of the sensor reached a maximum value of NO_3^--N (approximately 104 ppm), after which the sensor response began to decay to less than 10 ppm of NO_3^--N due to water evaporation. Further, sensor 2 was kept in the same soil without the addition of water for approximately 2 weeks, and the concentration variability was investigated (Fig. 6e). The soil become parched without the addition of water and NO_3^--N solution. Under this condition, however, the sensor still exhibited a low ppm of nitrate (approximately 10–2 ppm). Interestingly, the sensor response decreased from approximately 10 ppm to 3 ppm over a long period of time (13 days), but the sensor response was found to be irregular, perhaps because of the changing room temperature or humidity level.

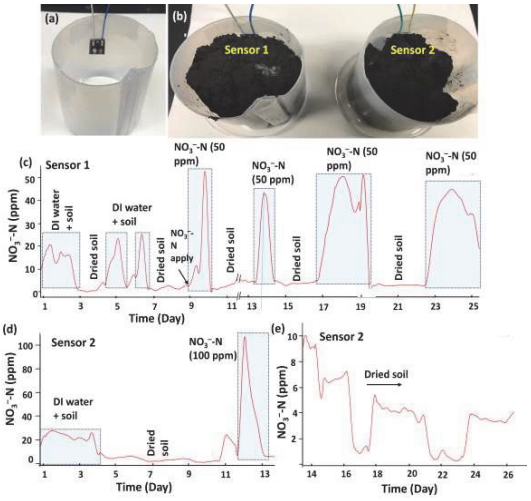

Figure 6. Long-term measurement with two sensors. Photographs of column beakers without soil slurries (a), and with soil slurries and sensor 1 and sensor 2 (b). For sensor 1 (c), the soil beaker was filled with DI water and then left to dry, and the soil slurry was again treated with water multiple times and then parched. Finally, DI water mixed with nitrate-nitrogen (50 ppm) was poured into the soil slurry in the column beaker with sensor 1 and left to dry. The process was repeated multiple times (for approximately 4 weeks) for sensor 1. For sensor 2, the soil slurry was initially filled with DI water, parched, and flushed with 100 ppm nitrate-nitrogen (d). After drying, sensor 2 was kept in the parched condition for about 2 w (e).

CONCLUSIONS

An all-solid-state miniature sensor designed for long-term use in continuous monitoring of soil nitrate was presented. The electro-activity properties of POT–MoS_2 composite were found to be excellent, and the material was used as an ion-to-electron transducing layer for nitrate detection in the sensor. The POT–MoS_2 composite material produced excellent sensor performance in terms of selectivity and sensitivity compared with MoS_2 and POT, and the reported nitrate sensors. This may be the result of the high lipophilicity and high redox properties of the POT–MoS_2 layer. The sensor is highly selectable with other anions and offers long-term stability. This sensor can be deployed into the soil for long-term nitrate monitoring. In the future, by replacing the ion selective membrane, the sensor can work to detect other soil nutrients, including potassium, phosphate, and sulfate, which will also help the phenotypic activity and nutrient uptake of plants [8]. With this evidence of sensor performance, the nitrate sensor may detect the variation in nitrate concentration in an agricultural setting [9]. This solid-state sensor may help farmers manage nitrogen fertilizer levels in fields to enhance crop yield.

ACKNOWLEDGEMENTS

The information, data, or work presented herein was funded in part by the Advanced Research Projects Agency-Energy (ARPA-E), U.S. Department of Energy, under Award Number DE-AR0000824. The views and opinions of authors expressed herein do not necessarily state or reflect those of the United States Government or any agency thereof. This project was also partially supported by the United State Department of Agriculture (USDA) under the grant number 2017-67013-26463, the National Science Foundation (NSF) under the grant number IOS-1650182, and the Plant Sciences Institute at Iowa State.

REFERENCES

[1] M.A. Ali, et al. "*In situ* integration of graphene foam–titanium nitride based bio-scaffolds and microfluidic structures for soil nutrient sensors." *Lab On A Chip*, 17.2 (2018): 274-285.

[2] V.I. Adamchuk, et al. "On-the-go soil sensors for precision agriculture." *Computers and Electronics in Agriculture*, 44.1 (2004): 71-91.

[3] P. SjoEberg, et al. "All-solid-state chloride-selective electrode based on poly (3-octylthiophene) and tridodecylmethylammonium chloride." *Electroanalysis*, 11.10-11 (1999): 821-824.

[4] J. Hu, et al. "Rational design of all-solid-state ion-selective electrodes and reference electrodes." *Trends in Analytical Chemistry* 76 (2016) 102-114.

[5] M. Cuartero, et al. "Tandem electrochemical desalination–potentiometric nitrate sensing for seawater analysis." *Analytical Chemistry,* 87.16 (2015) 8084-8089.

[6] T.A. Bendikov, et al. "Development and environmental application of a nitrate selective microsensor based on doped polypyrrole films." *Sensors and Actuators B. Chemical*, 106.2 (2005) 512-517.

[7] N. T. Garland, et al. "Flexible laser-induced graphene for nitrogen sensing in soil." *ACS Applied Materials Interfaces,* 10.45 (2018) 39124-39133.

[8] M.A. Ali, et al. "Microfluidic impedimetric sensor for soil nitrate detection using graphene oxide and conductive nanofibers enabled sensing interface." *Sensors and Actuators B. Chemical*, 239 (2017): 1289-1299.

[9] M.A. Ali, et al. "Tunable bioelectrodes with wrinkled-ridged graphene oxide surfaces for electrochemical nitrate sensors." *RSC Advances* 6.71 (2016): 67184-67195.

CONTACT

*Liang Dong, tel: +1- 515-294-0388; ldong@iastate.edu